ACS APPLIED MATERIALS & INTERFACES

Research Article

www.acsami.org

Polarization Rotation in Ferroelectric Tricolor $PbTiO_3/SrTiO_3/PbZr_{0.2}Ti_{0.8}O_3$ Superlattices

Nathalie Lemée,[*,§] Ingrid C. Infante,[#] Cécile Hubault,[§,†] Alexandre Boulle,[‡] Nils Blanc,[⊥,∥] Nathalie Boudet,[⊥,∥] Valérie Demange,[¶] and Michael G. Karkut[§]

[§]Laboratoire de Physique de la Matière Condensée, EA 2081, Université de Picardie Jules Verne, 80039 Amiens, France

[#]Laboratoire Structures, Propriétés et Modélisation des Solides, CentraleSupélec, CNRS-UMR 8580, Université Paris-Saclay, 92295 Cedex Châtenay-Malabry, France

[‡]Sciences des Procédés Céramiques et de Traitements de Surface, CNRS UMR 7315, Centre Européen de la Céramique, 87068 Limoges, France

[⊥]University of Grenoble Alpes, Institut NEEL, F-38000 Grenoble, France

[∥]CNRS, Institut NEEL, F-38042 Grenoble, France

[¶]Institut des Sciences Chimiques de Rennes, UMR 6226 CNRS/Université de Rennes 1, Campus de Beaulieu, 35042 Rennes, France

ABSTRACT: In ferroelectric thin films, controlling the orientation of the polarization is a key element to controlling their physical properties. We use laboratory and synchrotron X-ray diffraction to investigate ferroelectric bicolor $PbTiO_3/PbZr_{0.2}Ti_{0.8}O_3$ and tricolor $PbTiO_3/SrTiO_3/PbZr_{0.2}Ti_{0.8}O_3$ superlattices and to study the role of the $SrTiO_3$ layers on the domain structure. In the tricolor superlattices, we demonstrate the existence of 180° ferroelectric stripe nanodomains, induced by the depolarization field produced by the $SrTiO_3$ layers. Each ultrathin $SrTiO_3$ layer modifies the electrostatic boundary conditions between the ferroelectric layers compared to the corresponding bicolor structures, leading to the suppression of the a/c polydomain states. Combined with the electrostatic effect, the tensile strain induced by $PbZr_{0.2}Ti_{0.8}O_3$ in the $PbTiO_3$ layers leads to polarization rotation in the system as evidenced by grazing incidence X-ray measurements. This polarization rotation is associated with the monoclinic Mc phase as revealed by the splitting of the (HHL) and (H0L) reciprocal lattice points. This work demonstrates that the tricolor paraelectric/ferroelectric superlattices constitute a tunable system to investigate the concomitant effects of strains and depolarizing fields. Our studies provide a pathway to stabilize a monoclinic symmetry in ferroelectric layers, which is of particular interest for the enhancement of the piezoelectric properties.

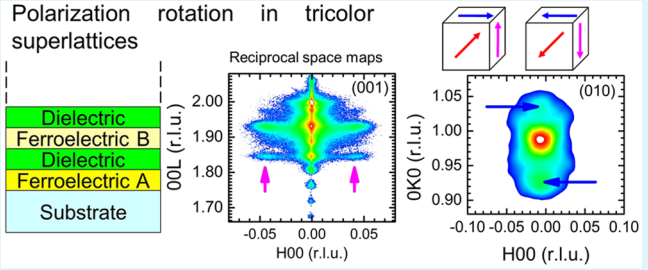

KEYWORDS: *ferroelectric materials, epitaxial and superlattice film, domain structure, strain and interface effects, Pb(Zr,Ti)O_3-based films*

1. INTRODUCTION

Ferroelectric thin films have demonstrated great potential for microelectronics applications. The dielectric, piezoelectric, and optical properties of ferroelectric thin films are strongly influenced by the domain structure.[1] Ferroic domain structures occur to minimize the elastic and the electrostatic energy of the film[2] and so the existence of a particular domain structure is directly controlled by both the strain and the electrostatic environment.[3] Strain and thus the elastic energy in the film can be relaxed by either the formation of 90° ferroelastic domains or by the appearance of misfit dislocations. Moreover, in order to minimize the electrostatic energy, 180° stripe domain structures can form consisting of alternate up and down polarization.[4] Although these stripe domain structures are generally associated with a reduction of the functional properties when compared to the monodomain state,[5,6] recent studies have demonstrated that ferroelastic domains as well as pure ferroelectric domains can lead to fascinating physical properties.[7,8] In ferroelectric thin films, the interplay between epitaxial strain and electrical polarization has been used to optimize the ferroelectric performance, leading to strain engineering.[9] Since the domain size scales as the square root of the thickness according to Kittel's law,[10] the density of domains and domain walls will be high in ultrathin films. Recently new concepts exploiting ferroelectric nanodomain structures have emerged such as gradient engineering,[7] polarization rotation engineering,[11] or domain wall engineering.[12] These new approaches demonstrate that the polydomain structure can contribute to enhance the ferroelectric properties in thin films or superlattices.

In this context, superlattices (SLs) can undoubtedly play an important role in controlling and manipulating ferroelectric

Received: April 21, 2015
Accepted: August 28, 2015
Published: August 28, 2015

DOI: 10.1021/acsami.5b03456
ACS Appl. Mater. Interfaces 2015, 7, 19906−19913

domain structures. By the periodic repetition of individual ultrathin ferroelectric layers of varying thicknesses, superlattices can provide a means to investigate domains on the nanoscale as well as the effect of possible coupling or decoupling of the constituent layers. Theoretical studies[13−15] have predicted the enhancement of the ferroelectric properties in different classes of SL structures. In the case of ferroelectric/paraelectric SLs, the functional properties can be tuned by adjusting the ratio of the ferroelectric to the paraelectric material.[16] Depending on the thickness of the layers, strong or weak coupling can take place between the ferroelectric layers and these are susceptible to produce changes on the various physical properties.[17,8,18] Recently Zubko et al. have shown that the nanoscale domain wall motion associated with the 180° domain structure in $PbTiO_3/SrTiO_3$ (PT/STO) SLs can lead to an enhancement of the dielectric permittivity.[19] In some $PbTiO_3/CaTiO_3$ SLs,[11] a polarization rotation was reported and associated with an enhancement of the dielectric constant and the piezoresponse. These results demonstrate that SLs can provide a tunable structure to explore the physics of nanodomains.

In previous works, we have reported on the domain structure in bicolor $PbTiO_3/PbZr_{0.2}Ti_{0.8}O_3$ (PT/PZT 20−80) SLs and in tricolor PT/STO/PZT 20−80 SLs.[20] We have shown that the insertion of an ultrathin layer of STO (1 nm thick) at each interface between PT and PZT 20−80 layers has inhibited the formation of 90° polydomain structures that occur in bicolor PT/PZT 20−80 SLs so as to relax the misfit strains. Here we present structural studies showing the role played by ultrathin STO layers on the control of the domain structure in tricolor SLs. We demonstrate (1) the existence of 180° ferroelectric stripe nanodomains which are induced by the depolarizing field produced by the STO layers and (2) the polarization rotation resulting from the tensile strains occurring due to the particular combination of PT, PZT, and STO in these tricolor SLs. An enhancement of the piezoelectric properties is reported in the literature for such monoclinic symmetry.[11,21] Therefore, the development of such tricolor SLs is of particular interest, not only for the fundamental understanding of the interaction between strain and electrostatic contributions, but also for their potential in improving the piezoelectric performance.

2. EXPERIMENTAL DETAILS

The superlattices were grown on single crystal (001) $SrTiO_3$ (STO) substrates, by pulsed laser deposition using a KrF excimer laser (λ = 248 nm) and ceramic targets of $Pb_{1.1}TiO_3$ (PT) and $Pb_{1.1}(Zr_{0.2}Ti_{0.8})O_3$ (PZT 20/80) and $SrTiO_3$. The substrates were chemically treated and annealed to obtain a TiO_2 termination, following the procedure described by Koster et al.[22] The PT, PZT 20/80, and STO layers were deposited at a substrate temperature of 650 °C in 0.1 mbar of oxygen, with a laser fluence of 2 $J.cm^{-2}$ and a pulse rate of 2 Hz. The deposition system is equipped with a 15 kV reflection high energy electron diffraction (RHEED) system which was used to control the surface quality of the substrate, and the first and the last layers of the superlattice. The superlattices are designated hereafter $[PT_p/PZT_z]_x$ or $[PT_p/STO_s/PZT_z/STO_s]_x$ where p, z, or s indicate the number of unit cells of each material and x corresponds to the number of periods in the superlattice.

Room temperature structural analysis was performed on a D8 Advance Bruker diffractometer (Cu K_α radiation, 1.5418 Å) and on a high resolution D8 Discover Bruker diffractometer (Cu $K_{\alpha1}$ radiation, 1.5406 Å). The reciprocal space map recorded around the (002) reflection of the substrate and presented hereafter is plotted in reciprocal-lattice units (rlu) with respect to the substrate lattice parameter (a_{STO} = 3.905 Å). The temperature X-ray diffraction (XRD) measurements were carried out from room temperature up to 725 °C in air using an in-house designed goniometer permitting high-resolution measurements. These studies were done using monochromatic Cu $K_{\alpha1}$ radiation issued from an 18 kW rotating anode (Rigaku). The maximum temperature was imposed so as to avoid any degradation of the samples. All the measurements were reproducible after thermal cycling. The lattice parameters were determined by fitting XRD scans around the (002) reflection (out-of-plane lattice parameter) or around the (103) reflection (in-plane lattice parameter). For a superlattice with a period Λ of n unit cells, the average out-of-plane lattice parameter was calculated from the n^{th} peak of the superlattice along the [00l] direction. To investigate the in-plane polar structure, grazing incidence in-plane X-ray diffraction was carried out at ESRF-BM2 (Grenoble, France). The energy of the X-ray radiation was fixed at 10 keV (1.2398 Å). Reciprocal space maps (RSMs) around different (HK0) reflections were investigated. The satellite peaks around the (100), (010), and (110) reflections were measured at a grazing incidence angle of 0.5°.

3. RESULTS AND DISCUSSION

The relation between the ferroelectric transition temperature with the domain structure is well established (see for example ref 23). To situate the behavior of the tricolor SL, we present in Figure 1 the temperature dependence of the average out-of-plane lattice parameter (c-axis) for the tricolor ($[PT_9/STO_2/PZT_{10}/STO_2]_{20}$), along with the bicolor mono-($[PT_2/PZT_2]_{20}$) and polydomain ($[PT_{10}/PZT_{11}]_{20}$) SLs.

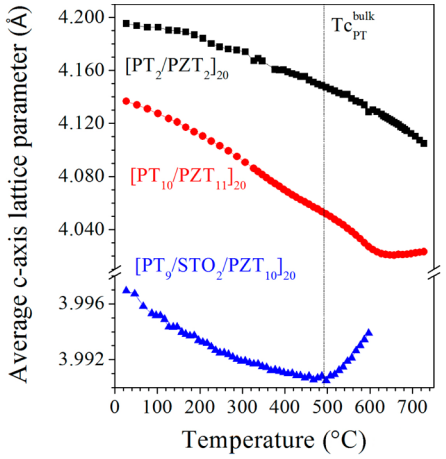

Figure 1. Temperature dependence of the average out-of-plane c axis lattice parameter for three SLs: $[PT_2/PZT_2]_{20}$, $[PT_{10}/PZT_{11}]_{20}$, and $[PT_9/STO_2/PZT_{10}/STO_2]_{20}$. The dotted line indicates the Curie temperature of bulk PT. Note the break in the vertical axis.

We have previously determined that the $[PT_2/PZT_2]_{20}$ superlattice[24] and the $([PT_9/STO_2/PZT_{10}/STO_2]_{20}$ superlattice[20] are purely c-axis oriented, whereas the $[PT_{10}/PZT_{11}]_{20}$ sample is characterized by a 90° a/c polydomain structure.[24] Table 1 summarizes the structural parameters corresponding to these SLs. In Figure 1, we observe the decrease of the c-axis lattice parameter related to the reduction of the out-of-plane component of polarization on approaching the ferroelectric transition. It is clear that the Curie temperature, T_C, is significantly less in the tricolor sample than that of the two bicolor SLs.

To explore this situation further, we consider the in-plane lattice parameter for these samples. Starting with the bicolor $[PT_{10}/PZT_{11}]_{20}$ sample, the in-plane lattice parameter is 3.985 Å at 607 °C close to T_C and 3.935 Å at room temperature. This superlattice is partially strained to the substrate (a = 3.905 Å),

DOI: 10.1021/acsami.5b03456
ACS Appl. Mater. Interfaces 2015, 7, 19906−19913

Table 1. Structural Parameters Determined at Room Temperature and Close to the Deposition Temperature for Different Types of Superlattices[a]

sample	domains	$d_{\parallel}$ (Å) (25 °C)	$d_{\perp}/d_{\parallel}$ (25 °C)	$d_{\parallel}$ (Å) (temp °C)	$d_{\perp}/d_{\parallel}$ (temp °C)
$[PT_{10}/PZT_{11}]_{20}$	a/c	3.935	1.05	3.985 (607 °C)	1.010 (607 °C)
$[PT_2/PZT_2]_{20}$	c	3.905	1.08	3.936 (727 °C)	1.040 (727 °C)
$[PT_9/STO_2/PZT_{10}]_{20}$	c	3.959	1.01	3.988 (607 °C)	1.009 (607 °C)

[a] $d_{\perp}$ and $d_{\parallel}$ represent the average out-of-plane and the in-plane lattice parameter, respectively. We note that the parameter value of cubic STO substrate is a_{STO} (25 °C) = 3.905 Å and a_{STO} (727 °C) = 3.932 Å.

since the strain starts to relax at the center of the first PZT 20−80 layer as observed by high resolution transmission electron microscopy.[24] Despite this strain relaxation induced by the a/c polydomain formation, the Curie temperature is still significantly higher than the value reported for bulk PT (493 °C)[25] and PZT 20−80 (460 °C),[25] meaning that the strain relaxation is only partial. We have previously demonstrated in these bicolor SLs that as the period, as well as the total thickness, is reduced, the compressive strain induced by the substrate becomes stronger[24] and the monodomain state becomes more energetically favorable. As a consequence, the domain structure can evolve from 90° polydomain to pure c domain, as we in fact observe in the $[PT_2/PZT_2]_{20}$ SL, whose in-plane lattice parameter of 3.905 Å at room temperature (Table 1) indicates that the SL is fully strained to the substrate. We detect no ferroelectric transition up to a maximum temperature of 725 °C for this SL. This upward shift in T_C is in good agreement with reported data that relates the increase of the T_C with compressive strain.[26−28] As to the trilayer $[PT_9/STO_2/PZT_{10}/STO_2]_{20}$ sample, the temperature dependence of the lattice parameter compared to that of the bilayer SLs is striking. We note that the bicolor $[PT_{10}/PZT_{11}]_{20}$ and the tricolor $[PT_9/STO_2/PZT_{10}/STO_2]_{20}$ SLs have a comparable number of unit cells within the ferroelectric layers and that the sole difference between the two is the presence of two unit cells of STO at each PT/PZT 20−80 interface in the tricolor sample. As we have previously reported, evidence from XRD and transmission electron microscopy[20] shows that the insertion of the ultrathin layer of STO strongly modifies the domain structure in the superlattice and suppresses the 90° a/c polydomain formation. The comparison of the *c*-axis temperature evolution for these two types of superlattices demonstrates that the ferroelectric transition is strongly influenced by the presence of the paraelectric layer in the stacking structure. We note that for these two samples the ferroelectric transition is continuous second order, a commonly observed consequence of the epitaxial strain in ferroelectric thin films and SLs. The evolution of the out-of-plane lattice parameter for the tricolor SL is quite soft and despite the pure *c*-axis orientation, the Curie temperature is ∼500 °C and thus very similar to the reported T_C of 493 °C for bulk PT. The significant reduction of the measured average out-of-plane lattice parameter of the tricolor SLs compared to the bicolor ones, points to a weak out-of-plane component of the polarization in the tricolor systems. Considering the strain state of these SLs via the in-plane lattice parameter given in Table 1, we note that for the tricolor sample it is appreciably larger ($d_{\parallel}$ = 3.959 Å at room temperature) than the substrate parameter (a_{STO} = 3.905 Å), indicating that partial strain relaxation occurs in this SL. Interestingly, the in-plane lattice parameter for this tricolor SL determined in the vicinity of the deposition temperature ($d_{\parallel}$ (607 °C) = 3.988 Å) indicates that the PT layer is under tensile strain (a_{PT} (607 °C) = 3.963 Å),[29] while the PZT layer is under compressive strain (a_{PZT} (607 °C) = 4.017 Å).[29] In contrast to this, in the bicolor $[PT_2/PZT_2]_{20}$ sample, the PT and PZT layers are both under compressive strain since the SL has been coherently grown on the substrate.

A Curie temperature close to the bulk value as observed in the tricolor SL is not common even when tensile strain has been induced[30] in the film. However, bulk-like value has been reported in *c*-axis oriented thin films[4,31] and more recently in ferroelectric/paraelectric PT-based SLs:[19,18] their common feature being a 180° stripe domain structure. The relation between the occurrence of 180° domains with a bulk-like T_C has also been justified theoretically.[32,33] These stripe structures consist of an in-plane periodic arrangement within the layers characterized by alternating up and down polarization. The formation of this stripe domain pattern reduces the depolarizing field when the screening by free charges is not efficient. It is strongly dependent on film thickness (the depolarizing field is larger in thinner films) and boundary conditions (more or fewer free charges in short or open circuit conditions, respectively).[2] In the tricolor PT/STO/PZT SLs, each ultrathin STO layer modifies the boundary conditions between the ferroelectric layers compared to the equivalent bicolor structure. A change in the electrostatic coupling between the ferroelectric layers can therefore account for the decrease in the T_C value observed in Figure 1. Our synchrotron results rule out the presence of a stripe domain structure in the bicolor *c*-oriented $[PT_2/PZT_2]_{20}$ superlattice. This indicates a monodomain configuration for this sample, and thus highlights the role of the STO layer in producing the 180° domain patterns in the tricolor superlattices.

The stripe domain structure gives rise to an in-plane modulation of the structure factor, depending on whether the polarization in the domain is pointing up or down along the growth direction.[4] This in-plane modulation can be detected by an XRD scan perpendicular to the domain walls. Figure 2 shows the reciprocal space map recorded around the (002) reflection of the substrate, where in addition to the out-of-plane periodicity along the growth [001] direction related to the SL stacking, an in-plane modulation is clearly detected along the [100] direction. This in-plane modulation can be attributed to the presence of a 180° stripe domain structure,[19] with only the first order satellites being detected.[19,34] However, such in-plane modulation could also be produced by an ordered arrangement of dislocations, periodic structural defects or ferroelastic a-domains.[35−37] Transmission electron microscopy studies as well as reciprocal space mapping have excluded the presence of ferroelastic domains in the tricolor SLs.[20] To rule out the other possible non polar sources of periodic modulations, we present in Figure 3 the temperature dependence of the XRD profile of the satellite peaks.

The satellite peaks disappear on approaching the ferroelectric transition. This confirms the polar origin of this modulation, the intensity being indeed proportional to the square of the

DOI: 10.1021/acsami.5b03456
ACS Appl. Mater. Interfaces 2015, 7, 19906−19913

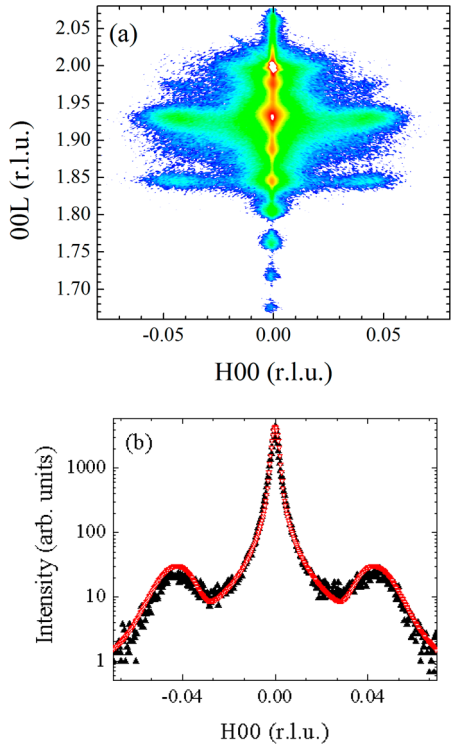

Figure 2. (a) RSM around the (002) reflection of a tricolor $[PT_9/STO_2/PZT_{10}/STO_2]_{20}$ SL. (b) The corresponding diffraction profile along the [H00] direction (in black) points out an in-plane modulation, characteristic of a 180° stripe domain structure and the profile fitting (in red) from which a stripe period of about 90 Å is determined.

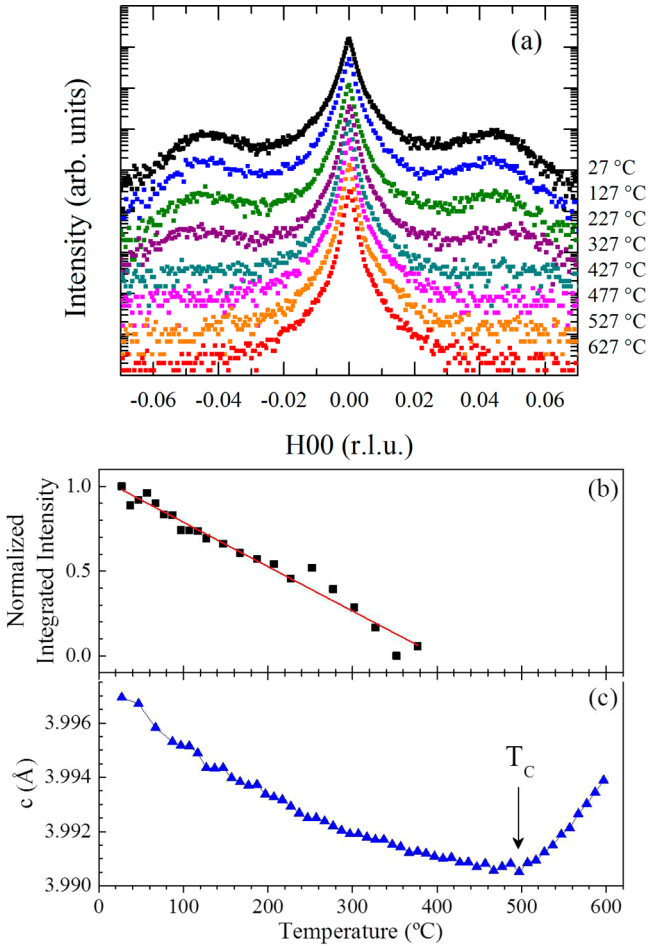

Figure 3. (a) Temperature dependence of the X-ray diffraction profile related to the in-plane modulation, around the (002) reflection of a $[PT_9/STO_2/PZT_{10}/STO_2]_{20}$ SL. (b) Corresponding temperature evolution of the integrated intensity of the satellite peaks. A Curie temperature of 450 °C is determined from a linear fit. (c) For comparison the temperature evolution of the average out-of-plane lattice parameter (c) for this tricolor SL.

polarization.[31] From a linear fit of the integrated intensity of the satellite peaks (Figure 3b), we determine a transition temperature of 450 °C for the 180° stripe domain structure, which is lower than the Curie temperature determined from the temperature dependence of the out-of-plane lattice parameter shown in Figure 3c (T_C = 500 °C). The discrepancy between these two values has also been reported in refs 18 and 30 and is probably because of the lower sensitivity of the integrated intensities compared to the high resolution X-ray peak position measurements. We note that the absence of even-order satellites is indicative of a 1:1 ratio of positive and negative domains.[4] We have developed a model, which allows us to simulate the type of diffuse X-ray scattering profile presented in Figures 2 and 3a, to determine structural parameters, such as the domain period, the polarization, and the domain wall thickness. The details of these calculations will be presented in a separate article. It solely relies on the presence of strain and the morphology of the stripe domain structure.

For the $[PT_9/STO_2/PZT_{10}/STO_2]_{20}$ SL, the stripe domain period at room temperature is ~90 Å. The domain size is defined by the minimization of the energy costs of the domains and the domain walls.[2] It has been clearly established that the stripe domain width scales with the square root of the film thickness in agreement with Kittel's law.[31,4,34] In ferroelectric-paraelectric SLs, this dependence is limited to the thickness of the individual ferroelectric layers or to the thickness of a couple of periods, depending on the nature of the electrostatic interactions (strong or weak ones) between the ferroelectric layers across the paraelectric interface.[8] As a consequence, the size of the domains is reduced in superlattices compared to the values reported in thin films.[4,38]

In our tricolor superlattices, additional studies are required to determine precisely the nature of the interactions between the different ferroelectric PT and PZT 20−80 layers. The condition for weak coupling reported by Stephanovich et al.,[17] is that the superlattice wavelength Λ is larger than the domain size, whereas for strong coupling to occur the domain size should be greater than Λ. Since Λ = 84 Å for the tricolor SL is almost twice as large as the domain size for all temperatures, we tentatively (since the situation is more complicated here than that treated by Stephanovich et al.[17]) suggest that the coupling between the layers is weak.

The reduced out-of-plane lattice parameter, as well as the tensile strain induced in the SL structure, could be a consequence of a rotation of the polarization. In order to investigate the in-plane polar structure, in-plane RSMs around the (100), (010), and (110) reflections were recorded using grazing incidence synchrotron radiation diffraction. The analysis of the in-plane distribution of the satellites, produced by the 180° stripe domain structure enables us to determine the orientation of the polarization. We present in Figure 4 different

DOI: 10.1021/acsami.5b03456
ACS Appl. Mater. Interfaces 2015, 7, 19906−19913

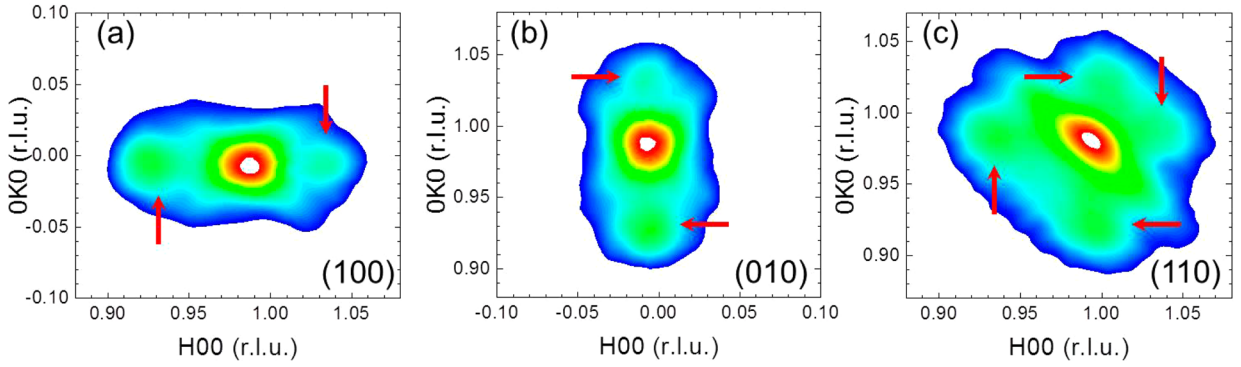

Figure 4. Grazing incidence X-ray diffraction RSMs measured for the $[PT_9/STO_2/PZT_{10}/STO_2]_{20}$ tricolor SL, around the (a) (100) and (b) (010) reflections, and (c) the diffraction profile along the [110] direction. The arrows indicate the satellite peaks.

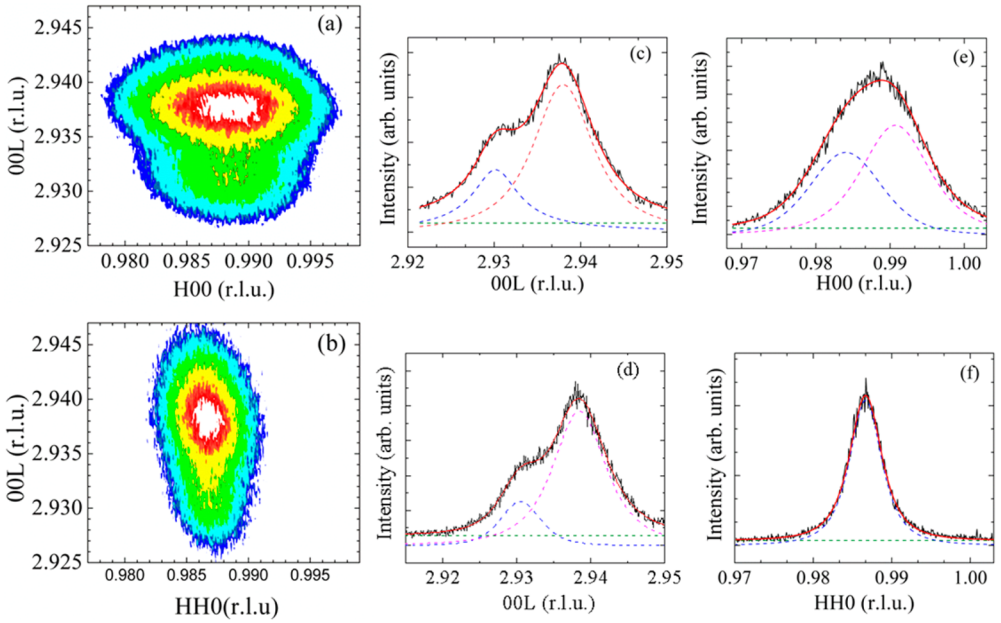

Figure 5. X-ray diffraction reciprocal space maps around (a) the (103) and (b) the (113) reflections of the $[PT_9/STO_2/PZT_{10}/STO_2]_{20}$ tricolor superlattice. The splitting is highlighted by the 1D cross sections presented: (c and d) along the longitudinal direction for $H = 0.987$ for the (103) and (113) reflection, respectively; (e and f) along the transversal direction for $L = 2.938$ for the (103) and (113) reflection, respectively. The dashed lines represent the fitting curves used to fit the XRD section profile (red solid curve). A M_C monoclinic phase is clearly evidenced by the 3-fold splitting observed around the (103) reflection. These measurements were carried out on a Bruker Discover diffractometer with Cu $K_{\alpha 1}$ radiation.

RSMs recorded around the (HK0) reflections for a $[PT_9/STO_2/PZT_{10}/STO_2]_{20}$ tricolor SL. Each RSM shows in-plane satellites, whose period Λ (Λ = 85 Å) is consistent with the polar modulation measured around the specular reflections. Since satellite peaks of similar periods are detected around the (H00), (0K0), and (HH0) reflections, we conclude that the polarization in the domain structure has in-plane components. The detection of in-plane and out-of-plane components of the polarization is strong evidence for the existence of a rotational phase characterized by a polarization rotation away from the normal. Such polarization rotation has been already reported by Catalan et al.[39] for an ultrathin film of PT (5 nm thick), and by Sinsheimer et al.[11] for $PT/CaTiO_3$ superlattices.

The rotation of the polarization should result in a monoclinic distortion[11] which can be evidenced by the splitting of the (HHL) and (H0L) reflections. Depending on the type of splitting, it is possible to discriminate between the three monoclinic phases (M_A, M_B, M_C), each being characterized by a different polarization orientation.[40] We present the RSMs and the corresponding 1D cross sections taken about the (103) and (113) peaks in the tricolor superlattices in Figure 5.

The 3-fold and 2-fold splitting detected respectively around the (103) and (113) reflections, are consistent with a M_c phase. It implies that the polarization is directed along the [u0v] directions in the pseudocubic coordinates. The splitting along the L direction allows the calculation of the distorted angle β which is close to 89.8°. This monoclinic distortion confirms the polarization rotation and thus the existence of satellites around in-plane Bragg peaks related to in-plane 180° stripe domains (Figure 4). Furthermore, it helps to explain the reduced out-of-plane lattice parameter detected in the tricolor SLs. Figure 6 illustrates the domain orientations expected in a M_c monoclinic symmetry and compatible with the modulation detected in the in-plane and out-of-plane RSM presented above.

This type of M_c monoclinic distortion was also reported in ferroelectric $PT/CaTiO_3$ SLs.[11] Enhancement of the piezoelectric response and the dielectric constant is associated with this change of symmetry. The monoclinic symmetry reported

DOI: 10.1021/acsami.5b03456
ACS Appl. Mater. Interfaces 2015, 7, 19906−19913

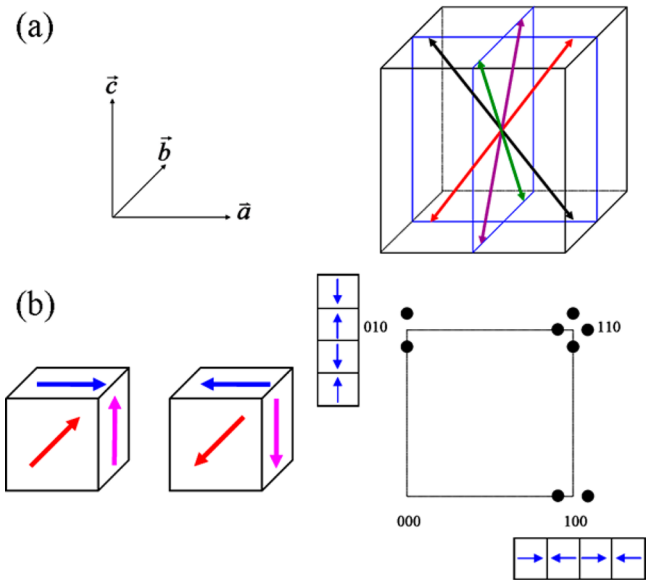

Figure 6. (a) Schematic representation of the possible orientation states in the monoclinic M_c phase. The arrows indicate the possible direction of the spontaneous polarization. (b) For one orientation state, representation of the spontaneous polarization (in red) and its projection on the {001} pseudocubic planes (in blue and pink) (on the left). Schematic drawings of the corresponding reciprocal space maps and domain configurations are on the right.

by Sinsheimer et al.[11] was shown to result from a competition between the direction for polarization in PT under compressive strain ([001] direction) and $CaTiO_3$ under tensile strain ([110] direction). This distortion was detected for a specific range of $CaTiO_3$ volume fraction.

In our tricolor SLs, even if the strain parameter contributes to the rotation of the polarization, it cannot be considered as the sole factor, since the strain state is very similar in the bicolor and the tricolor superlattices. Here, the insertion of the dielectric STO layer between the ferroelectric layers has probably enhanced the depolarizing field within the SL. Such increase of the depolarizing field induced by STO layers has been clearly demonstrated in PT thin films.[41] Consequently the STO layer acts as a means to modify the boundary conditions and is thus at the origin of the stripe nanodomain structure.

In polydomain PT/STO superlattices, the rotation of the local polarization vector across the domain walls joining two 180° domains has been proposed by first-principles calculations,[42] as well as by ultrahigh resolution electron energy loss spectroscopy observations.[8] The polarization rotation is primarily associated with a large in-plane shift of the Pb atoms in the PbO layers in the vicinity of the interface[42] and allows the confinement of the polarization flux within the ferroelectric layers. This in-plane polarization couples to the in-plane strain induced by the domain walls in the 180° pattern.[42] In our tricolor superlattices, the offset of opposite domains can also contribute in the same way to the local rotation of the polarization vector. As reported in a polydomain a/c dislocation free PT thin film,[7] a transverse strain gradient due to the bending of domain walls can induce horizontal flexoelectricity, which results in an in-plane component of the electric polarization in the c-domains. In the tricolor samples, there is no polydomain a/c structure and so there will be no twinning structure contribution to an in-plane strain gradient. However, another factor that might affect the local polarization configuration is an in-plane flexoelectric effect produced by the strain gradients associated with the 180° polydomain configurations. Nevertheless, it is probably not the primary driving force giving rise to the change in symmetry, since no symmetry lowering is attached to the local rotation of the polarization vector neither in PT/STO superlattices[8] nor in the polydomain a/c PT thin film.[7]

The large tensile strain induced in the ferroelectric PT layers by the PZT 20−80 layers is also going to play a role through the strain-polarization coupling. Symmetry lowering was reported from first-principles calculations for the case of partially relaxed $BaTiO_3/SrTiO_3$ superlattices.[43] In these structures, the STO and $BaTiO_3$ layers were under in-plane tensile strain and in-plane compressive strain, respectively. These calculations demonstrate that a polarization component in the [110] direction can take place in the STO layers which thus contributes to the rotation of the polarization in the superlattice leading to the monoclinic symmetry.[43] In the BTO layers the polarization develops along the [001] direction because of the compressive strain. The competition between these two polarization components, resulting from varying $BaTiO_3/SrTiO_3$ ratio, was reported to control the orientation of the polarization. In our tricolor superlattices, the PZT is compressively strained at high temperatures which can lead to an out of plane polarization on cooling, and both STO and PT are under tensile strain. Thus, in the tricolor SLs, there is the possibility of competition between different polarization orientations through different strain states in the layers, and this should be considered as a possible explanation for the polarization rotation and the associated monoclinic symmetry that we present here. The monoclinic phase results from a combination of the electrostatic and the strain effects, and of course, a first-principles study of this complex system would help clarify some of the fundamental points raised in this work.

4. CONCLUSION

In conclusion, we have shown that a polarization rotation in ferroelectric/paraelectric tricolor superlattices based on PT, PZT 20−80 and STO can be achieved through the combination of tensile strain and enhanced depolarizing field. This work shows also that the tricolor geometry of the superlattices offers a good opportunity to tune the strain and thus functional properties through the structural and electrical mismatch between the different materials involved in the superlattice. The role of the paraelectric layer is crucial in inducing the stripe nanodomain structure inhibiting the 90° polydomain relaxation, whereas the polarization is rotated primarily by the effect of tensile strain which is induced by the combination of different ferroelectric layers. Such tricolor superlattices constitute an ideal system to investigate the strain effects as well as the electrostatic interactions between different ferroelectric materials. The ferroelectric/paraelectric tricolor superlattices offer an effective pathway to stabilize a rotation of the polarization, compatible with an enhancement of the piezoelectric properties.

AUTHOR INFORMATION

Corresponding Author

*E-mail: nathalie.lemee@u-picardie.fr.

DOI: 10.1021/acsami.5b03456
ACS Appl. Mater. Interfaces 2015, 7, 19906−19913

Present Address

†C.H.: Toyota Technological Institute, Energy Materials Laboratory, 2-12-1 Hisakata, Tempaku-ku, Nagoya 468-8511, Japan

Notes

The authors declare no competing financial interest.

■ ACKNOWLEDGMENTS

This work is supported by the Region of Picardie and the European Social Fund. I.C.I. thanks the French ANR program NOMILOPS (ANR-11-BS10-016-02) project for financial support. N.L. thanks Prof. I. Lukyanchuk for useful discussions. N.L. and V.D. are grateful to Dr A. Perrin for his precious aid with the room-temperature XRD measurements.

■ REFERENCES

(1) Dawber, M.; Rabe, K. M.; Scott, J. F. Physics of Thin Film Ferroelectric Oxides. *Rev. Mod. Phys.* **2005**, *77* (4), 1083−1130.

(2) Catalan, G.; Seidel, J.; Ramesh, R.; Scott, J. F. Domain Wall Nanoelectronics. *Rev. Mod. Phys.* **2012**, *84* (1), 119−156.

(3) Kornev, I.; Fu, H.; Bellaiche, L. Ultrathin Films of Ferroelectric Solid Solutions under a Residual Depolarizing Field. *Phys. Rev. Lett.* **2004**, *93* (19), 196104.

(4) Streiffer, S. K.; Eastman, J. A.; Fong, D. D.; Thompson, C.; Munkholm, A.; Ramana Murty, M. V.; Auciello, O.; Bai, G. R.; Stephenson, G. B. Observation of Nanoscale 180° Stripe Domains in Ferroelectric $PbTiO_3$ Thin Films. *Phys. Rev. Lett.* **2002**, *89* (6), 067601.

(5) Takahashi, R.; Grepstad, J. K.; Tybell, T.; Matsumoto, Y. Photochemical Switching of Ultrathin $PbTiO_3$ Films. *Appl. Phys. Lett.* **2008**, *92*, 112901.

(6) Lichtensteiger, C.; Triscone, J.-M.; Junquera, J.; Ghosez, P. Ferroelectricity and Tetragonality in Ultrathin $PbTiO_3$ Films. *Phys. Rev. Lett.* **2005**, *94* (4), 047603−047606.

(7) Catalan, G.; Lubk, A.; Vlooswijk, A. H. G.; Snoeck, E.; Magen, C.; Janssens, A.; Rispens, G.; Rijnders, G.; Blank, D. H. A.; Noheda, B. Flexoelectric Rotation of Polarization in Ferroelectric Thin Films. *Nat. Mater.* **2011**, *10* (12), 963−967.

(8) Zubko, P.; Jecklin, N.; Torres-Pardo, A.; Aguado-Puente, P.; Gloter, A.; Lichtensteiger, C.; Junquera, J.; Stéphan, O.; Triscone, J.-M. Electrostatic Coupling and Local Structural Distortions at Interfaces in Ferroelectric/Paraelectric Superlattices. *Nano Lett.* **2012**, *12* (6), 2846−2851.

(9) Schlom, D. G.; Chen, L.-Q.; Eom, C.-B.; Rabe, K. M.; Streiffer, S. K.; Triscone, J.-M. Strain Tuning of Ferroelectric Thin Films. *Annu. Rev. Mater. Res.* **2007**, *37* (1), 589−626.

(10) Schilling, A.; Adams, T. B.; Bowman, R. M.; Gregg, J. M.; Catalan, G.; Scott, J. F. Scaling of Domain Periodicity with Thickness Measured in $BaTiO_3$ Single Crystal Lamellae and Comparison with Other Ferroics. *Phys. Rev. B: Condens. Matter Mater. Phys.* **2006**, *74* (2), 024115.

(11) Sinsheimer, J.; Callori, S. J.; Bein, B.; Benkara, Y.; Daley, J.; Coraor, J.; Su, D.; Stephens, P. W.; Dawber, M. Engineering Polarization Rotation in a Ferroelectric Superlattice. *Phys. Rev. Lett.* **2012**, *109* (16), 167601.

(12) Wada, S.; Yako, K.; Yokoo, K.; Kakemoto, H.; Tsurumi, T. Domain Wall Engineering in Barium Titanate Single Crystals for Enhanced Piezoelectric Properties. *Ferroelectrics* **2006**, *334* (1), 17−27.

(13) Aguado-Puente, P.; García-Fernández, P.; Junquera, J. Interplay of Couplings between Antiferrodistortive, Ferroelectric, and Strain Degrees of Freedom in Monodomain $PbTiO_3/SrTiO_3$ Superlattices. *Phys. Rev. Lett.* **2011**, *107* (21), 217601.

(14) Lee, H. N.; Christen, H. M.; Chisholm, M. F.; Rouleau, C. M.; Lowndes, D. H. Strong Polarization Enhancement in Asymmetric Three-Component Ferroelectric Superlattices. *Nature* **2005**, *433* (7024), 395−399.

(15) Nakhmanson, S. M.; Rabe, K. M.; Vanderbilt, D. Polarization Enhancement in Two- and Three- Component Ferroelectric Superlattices. *Appl. Phys. Lett.* **2005**, *87* (10), 102906.

(16) Dawber, M.; Stucki, N.; Lichtensteiger, C.; Gariglio, S.; Ghosez, P.; Triscone, J.-M. Tailoring the Properties of Artificially Layered Ferroelectric Superlattices. *Adv. Mater.* **2007**, *19* (23), 4153−4159.

(17) Stephanovich, V. A.; Luk'yanchuk, I. A.; Karkut, M. G. Domain-Enhanced Interlayer Coupling in Ferroelectric/Paraelectric Superlattices. *Phys. Rev. Lett.* **2005**, *94* (4), 047601.

(18) Zubko, P.; Jecklin, N.; Stucki, N.; Lichtensteiger, C.; Rispens, G.; Triscone, J.-M. Ferroelectric Domains in $PbTiO_3/SrTiO_3$ Superlattices. *Ferroelectrics* **2012**, *433* (1), 127−137.

(19) Zubko, P.; Stucki, N.; Lichtensteiger, C.; Triscone, J.-M. X-Ray Diffraction Studies of 180° Ferroelectric Domains in $PbTiO_3/SrTiO_3$ Superlattices under an Applied Electric Field. *Phys. Rev. Lett.* **2010**, *104* (18), 187601.

(20) Hubault, C.; Davoisne, C.; Dupont, L.; Perrin, A.; Boulle, A.; Holc, J.; Kosec, M.; Karkut, M. G.; Lemée, N. Inhibition of Polydomain Formation in $PbTiO_3/PbZr_{0.2}Ti_{0.8}O_3$ Superlattices by Intercalation of Ultra-Thin $SrTiO_3$ Layers. *Appl. Phys. Lett.* **2011**, *99* (5), 052905.

(21) Wu, Z.; Cohen, R. E. Pressure-Induced Anomalous Phase Transitions and Colossal Enhancement of Piezoelectricity in $PbTiO_3$. *Phys. Rev. Lett.* **2005**, *95* (3), 037601.

(22) Koster, G.; Kropman, B. L.; Rijnders, G. J. H. M.; Blank, D. H. A.; Rogalla, H. Quasi-Ideal Strontium Titanate Crystal Surfaces through Formation of Strontium Hydroxide. *Appl. Phys. Lett.* **1998**, *73* (20), 2920−2922.

(23) Tagantsev, A.; Cross, E. L.; Fousek, J. *Domains in Ferroic Crystals and Thin Films*; Springer: Berlin, 2010.

(24) Hubault, C.; Davoisne, C.; Boulle, A.; Dupont, L.; Demange, V.; Perrin, A.; Gautier, B.; Holc, J.; Kosec, M.; Karkut, M. G.; Lemée, N. Strain Effect in $PbTiO_3/PbZr_{0.2}Ti_{0.8}O_3$ Superlattices: From Polydomain to Monodomain Structures. *J. Appl. Phys.* **2012**, *112* (11), 114102.

(25) Jona, F.; Shirane, G. *Ferroelectric Crystals*; Pergamon Press: New York, 1962.

(26) Janolin, P.-E.; Fraisse, B.; Le Marrec, F.; Dkhil, B. Partial Decoupling between Strain and Polarization in Mono-Oriented $Pb(Zr_{0.2}Ti_{0.8})O_3$ Thin Film. *Appl. Phys. Lett.* **2007**, *90* (21), 212904.

(27) Janolin, P.-E.; Le Marrec, F.; Chevreul, J.; Dkhil, B. Temperature Evolution of the Structural Properties of Monodomain Ferroelectric Thin Film. *Appl. Phys. Lett.* **2007**, *90* (19), 192910.

(28) Venkatesan, S.; Vlooswijk, A.; Kooi, B. J.; Morelli, A.; Palasantzas, G.; De Hosson, J. T. M.; Noheda, B. Monodomain Strained Ferroelectric $PbTiO_3$ Thin Films: Phase Transition and Critical Thickness Study. *Phys. Rev. B: Condens. Matter Mater. Phys.* **2008**, *78* (10), 104112.

(29) Janolin, P.-E., Instabilités Structurales sous Contraintes dans les Matériaux Ferroélectriques, Ph.D thesis, Ecole Centrale Paris, 2006.

(30) Bouyanfif, H.; Lemée, N.; El Marssi, M.; Le Marrec, F.; Dkhil, B.; Chevreul, J.; Fraisse, B.; Picot, J. C.; Karkut, M. G. $PbMg_{1/3}Nb_{2/3}O_3/PbTiO_3$ Superlattices: An X-Ray Diffraction and Raman Spectroscopy Temperature-Dependent Study. *Phys. Rev. B: Condens. Matter Mater. Phys.* **2007**, *76* (1), 014124.

(31) Fong, D. D.; Stephenson, G. B.; Streiffer, S. K.; Eastman, J. A.; Auciello, O.; Fuoss, P. H.; Thompson, C. Ferroelectricity in Ultrathin Perovskite Films. *Science* **2004**, *304* (5677), 1650−1653.

(32) De Guerville, F.; Luk'yanchuk, I.; Lahoche, L.; El Marssi, M. Modeling of Ferroelectric Domains in Thin Films and Superlattices. *Mater. Sci. Eng., B* **2005**, *120* (1−3), 16−20.

(33) Stephenson, G. B.; Elder, K. R. Theory for Equilibrium 180° Stripe Domains in $PbTiO_3$ Films. *J. Appl. Phys.* **2006**, *100* (5), 051601.

(34) Takahashi, R.; Dahl, O.; Eberg, E.; Grepstad, J. K.; Tybell, T. Ferroelectric Stripe Domains in $PbTiO_3$ Thin Films: Depolarization Field and Domain Randomness. *J. Appl. Phys.* **2008**, *104* (6), 064109.

(35) Kaganer, V. M.; Brandt, O.; Trampert, A.; Ploog, K. H. X-Ray Diffraction Peak Profiles from Threading Dislocations in GaN

DOI: 10.1021/acsami.5b03456
ACS Appl. Mater. Interfaces 2015, 7, 19906−19913

Epitaxial Films. *Phys. Rev. B: Condens. Matter Mater. Phys.* **2005**, *72* (4), 045423.
(36) Vlooswijk, A. H. G.; Noheda, B.; Catalan, G.; Janssens, A.; Barcones, B.; Rijnders, G.; Blank, D. H. A.; Venkatesan, S.; Kooi, B.; de Hosson, J. T. M. Smallest 90° Domains in Epitaxial Ferroelectric Films. *Appl. Phys. Lett.* **2007**, *91* (11), 112901.
(37) Vailionis, A.; Boschker, H.; Houwman, E.; Koster, G.; Rijnders, G.; Blank, D. H. A. Anisotropic Stress Relief Mechanism in Epitaxial $La_{0.67}Sr_{0.33}MnO_3$ Films. *Appl. Phys. Lett.* **2009**, *95* (15), 152508.
(38) Takahashi, R.; Dahl, O.; Eberg, E.; Grepstad, J. K.; Tybell, T. Ferroelectric Stripe Domains in $PbTiO_3$ Thin Films: Depolarization Field and Domain Randomness. *J. Appl. Phys.* **2008**, *104* (6), 064109.
(39) Catalan, G.; Janssens, A.; Rispens, G.; Csiszar, S.; Seeck, O.; Rijnders, G.; Blank, D. H. A.; Noheda, B. Polar Domains in Lead Titanate Films under Tensile Strain. *Phys. Rev. Lett.* **2006**, *96* (12), 127602.
(40) Christen, H. M.; Nam, J. H.; Kim, H. S.; Hatt, A. J.; Spaldin, N. A. Stress-induced R-M_A-M_C-T Symmetry Changes in $BiFeO_3$ Films. *Phys. Rev. B: Condens. Matter Mater. Phys.* **2011**, *83* (14), 144107.
(41) Lichtensteiger, C.; Fernandez-Pena, S.; Weymann, C.; Zubko, P.; Triscone, J.-M. Tuning of the Depolarization Field and Nanodomain Structure in Ferroelectric Thin Films. *Nano Lett.* **2014**, *14* (8), 4205−4211.
(42) Aguado-Puente, P.; Junquera, J. Structural and Energetic Properties of Domains in $PbTiO_3/SrTiO_3$ Superlattices from First Principles. *Phys. Rev. B: Condens. Matter Mater. Phys.* **2012**, *85* (18), 184105.
(43) Johnston, K.; Huang, X.; Neaton, J. B.; Rabe, K. M. First-Principles Study of Symmetry Lowering and Polarization in $BaTiO_3/SrTiO_3$ Superlattices with In-Plane Expansion. *Phys. Rev. B: Condens. Matter Mater. Phys.* **2005**, *71* (10), 100103.

DOI: 10.1021/acsami.5b03456
ACS Appl. Mater. Interfaces 2015, 7, 19906−19913